On the Occurrence of Competitive Adsorption at the Platinum−Acetonitrile Interface by Using Surface-Enhanced Raman Spectroscopy

Peigen Cao,[†] Yuhua Sun,[†] and Renao Gu*[,†]

Department of Chemistry, Suzhou University, Suzhou 215006, P. R. China, and State Key Laboratory for Physical Chemistry of Solid Surfaces, Department of Chemistry and Institute of Physical Chemistry, Xiamen University, Xiamen 361005, P. R. China

Received: December 27, 2002; In Final Form: April 12, 2003

Surface-enhanced Raman scattering (SERS) from the platinum electrode−acetonitrile interface in the presence of iodide, the lithium cation, water, and pyridine was analyzed as a function of applied potential. It was found that the typical Raman band of cyanide species by the dissociation of the solvent acetonitrile upon adsorption onto highly roughened platinum electrode surfaces was detectable for all of the systems that were studied. However, the onset potential of the dissociation reaction of acetontrile differed for the four systems. We assume that competitive adsorption may exist between each of the above four species and the solvent acetonitrile molecule, especially at the dissociation reaction−active sites of the Pt surface. This competitive adsorption therefore significantly inhibits the decomposition reaction of acetonitrile. The interactions of these adsorbates with Pt are assumed to weaken in the sequence pyridine > I^- > water ≈ Li^+ on the basis of the observations of different negative shifts of the onset potential of acetonitrile decomposition. For the system with water or iodide, double-band character for the CN band was also detected. It is assumed to be due to the existence of two types of adsorbed ion pairs at the Pt surface: $CN^-\cdots CH_3CN$ and $CN^-\cdots Li^+/Na^+$.

Introduction

Surface-enhanced Raman spectroscopy (SERS), first observed by Fleischmann et al. in 1974[1] and later confirmed by Jeanmaire and VanDuyne[2] and Albrecht and Creighton,[3] has stimulated considerable interest in the development of Raman spectroscopy as a technique for examining electrochemical interfaces.[4] Most of the SERS investigations were carried out in aqueous media. Only a few papers appearing in the literature were concerned with electrode−nonaqueous solution interfaces.[5−7] The structure and composition of the latter interface is undoubtedly strongly controlled by the behavior of nonaqueous solvents. Investigations of the solvent role in the double-layer region will help to clarify the nature of the electrode process occurring in these nonaqueous systems, for instance, electrochemical organic synthesis.

However, because of the low surface-detection sensitivity of Raman spectrometry in nonaqueous systems and interference from large quantity of organic solvents, reports on the SERS spectra of adsorbates from metal−nonaqueous solution interfaces are relatively few in the literature. Moreover, previous related studies were almost restricted to three well-known roughened coinage-metal surfaces: copper, silver, and gold. This undoubtedly impeded the development of the SERS technique as a versatile surface analytical tool applied particularly to nonaqueous solutions. Several methods have been employed successfully to extend in situ SERS to other transition metals such as platinum and iron[8−10] over the last two decades. These methods include the deposition of particles or thin layers of transition metals onto a SERS-active substrate (for instance, silver)[8,9] or the latter onto the former metal as a substrate.[10] The enhanced scattering of adsorbates on these transition-metal surfaces is normally assumed to originate from the long-range electromagnetic effect of SERS-active metals. This strategy has been employed to investigate the interactions of some organic inhibitors with iron.[8,9] However, because of the presence of the SERS-active metal, the interactions of the adsorbate with this metal surface may be reflected in the obtained spectrum and thus may bring about some ambiguities.

Recently, Weaver and co-workers[11] claimed that they had obtained pinhole-free ultrathin (three to five monolayers) films of Pt-group metals on gold by a judicious modification of the electrode deposition procedures. The strategy has been applied to the study of the adsorption of carbon monoxide on rhodium[12] and thiocyanate on platinum electrodes.[13] From recent studies in our laboratory, we have found that by applying special surface-roughening procedures for transition metals we can obtain a significant SERS signal of pyridine from bare platinum, nickel, and iron surfaces in aqueous solutions.[14−16] No deposition of SERS-active metals is needed. The adsorption behavior of pyridine,[15,16] benzotriazole,[17] and thiocyanate[18] on these transition-metal surfaces has been probed on the basis of the measured spectrum. The success in obtaining valuable in situ Raman scattering signals of adsorbates from aqueous media for transition metals stimulated us to extend this strategy to the electrode−nonaqueous solution interface. The adsorption and electro-oxidation of carbon monoxide at the platinum−acetonitrile interface has been investigated recently in our laboratory.[19]

As part of these ongoing studies, this paper deals mainly with the competitive adsorption occurring at the $Pt-CH_3CN$ interface. The role of the solvent acetonitrile has been analyzed on the basis of the measured spectra. Interesting results regarding the adsorption sequences of the adsorbates have been obtained.

* Corresponding author. E-mail: ragu@suda.edu.cn. Tel: 86+512+65112813, 65112645. Fax: 86+512+65231918.
[†] Suzhou University.
[‡] Xiamen University.

10.1021/jp027834j CCC: $25.00
Published on Web 05/23/2003

Experimental Section

Chemicals. The solvent acetonitrile (HPLC grade, 0.003% water) was distilled twice from calcium hydride and stored before use in sealed containers over Woelm alumina. Pyridine was of analytical reagent grade and was used without further purification. The anhydrous salts used in this work, lithium perchlorate and sodium iodide, were of analytical reagent grade and were dried by heating under vacuum up to 60 °C for 6 h before use.

Roughening Methods. An electrochemical oxidation−reduction cycle (orc) was applied to roughen the platinum electrode. Detailed information on the roughening procedure was described elsewhere.[19] What should be emphasized here is the possible existence of unstable atoms or clusters at the surface. They should be removed from the electrode surface to obtain a stable SERS-active substrate. This is of key importance in obtaining reproducible SER spectra of adsorbates. It is also an advantage of Pt over other SERS substrates. Additionally, because of the chemical inertness of the platinum metal, the roughened electrode can be reused several weeks later only after cycling the electrode in sulfuric acid solution for several minutes. After roughening the Pt electrode, it was immersed in acetonitrile solution prior to the Raman measurement to remove the contamination of water.

Raman Measurements. A three-compartment spectroelectrochemical cell was used to perform the in situ Raman measurements. The cell was dried in a vacuum oven at 120 °C before use. The working electrode was described above. A large Pt ring served as the counterelectrode. All of the potentials, unless otherwise specified, are reported versus a Ag/Ag^+ reference electrode in CH_3CN containing 0.1 M $LiClO_4$ and 0.01 M $AgNO_3$ (0.268 V versus a saturated calomel electrode, see ref 20). An EG&G model 173 potentiostat was employed to control the applied potential.

Raman spectra were recorded on a confocal microprobe Raman system (LabRam I from Dilor, France). Exciting radiation of wavelength 632.8 nm was provided by an inner air-cooled He−Ne laser with a power of 10 mW and a spot of size 3 μm at the sample surface. The slit and pinhole that were used were 200 and 800 μm, respectively. The acquisition time was 100 s, and each spectrum was measured three times. With a holographic notch filter and a CCD detector, it has an extremely high detecting sensitivity. A 50× long-working-length objective (8 mm) was used, so it was not necessary for the objective to be immersed in the solution.

Results and Discussion

Acetonitrile. First, we examined the behavior of acetonitrile as a solvent at the roughened platinum electrode surface. Previous studies[21] showed that the solvent may decompose at the catalytic roughened surface, yielding cyanide species, as characterized by the spectral features presented in Figure 1. The electrolyte was 0.1 M $LiClO_4/CH_3CN$. The two new bands located at ca. 2147 and 2115 cm^{-1}, which are not components of the Raman spectrum of free or coordinated acetonitrile,[22] exhibit similar frequency values and potential dependencies of the cyanide ion.[23] Hence, the presence of the new bands is reasonably attributed to the CN stretching mode of the decomposition product cyanide ion. This decomposition adsorption of acetonitrile has also been observed on copper and silver.[24,25] All of these observable decomposition reactions occur at roughened metallic surfaces. No dissociation of acetonitrile or reaction products such as CN^- were detected on smooth Pt(111) surfaces according to the studies of Norton and co-workers[26] and Villegas and Weaver.[27] Only agostic bond features (where no bonds are broken) of acetonitrile, for instance, the large red shift of CH stretches (30 cm^{-1}), were observed with infrared reflection absorption spectroscopy (IRRAS) by Norton et al.[26] In the studies of CO chemisorbed onto smooth polycrystalline Pt surfaces from acetonitrile solutions, the decomposition of acetonitrile was also not observed.[28,29] This may be caused by the different metallic surface features, with the roughened platinum surfaces used in the present study having highly catalytic properties. As is known to us, the roughened metal surface has many kinks, edges, and steps. These surface features probably facilitate the interaction and subsequent decomposition of acetonitrile on the roughened metal surfaces. However, when the flame-annealed Pt(111) sample was cooled above an aqueous solution of acetonitrile, the decomposition of acetonitrile into cyanide species was also detected by Dederichs and co-workers,[30] as evidenced by the appearance of the sum frequency generation band of cyanide. Another important finding in their studies is that the contamination of CO was observed upon changing the electrolyte to neat acetonitrile. The product CO was postulated to originate from the further oxidation of acetonitrile. However, in the present study, this phenomenon was not observed for the electrode potential being applied in the relatively negative potential region. Furthermore, the usually observed Pt−C bond associated closely with the adsorption of CO was not detectable throughout the potential region.

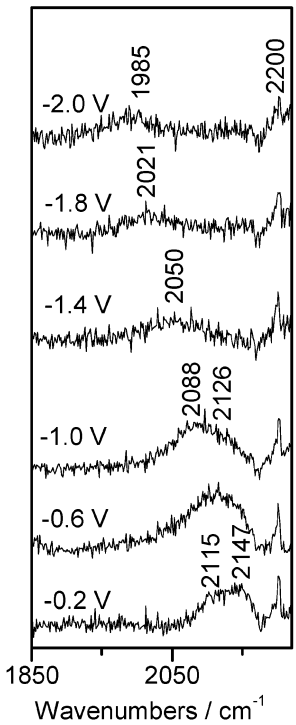

Figure 1. Representative potential-dependent SER spectra from a roughened platinum electrode in 0.1 M $LiClO_4$/acetonitrile.

The above discussions show that acetonitrile may decompose upon adsorption onto highly roughened platinum electrode surfaces. In addition, the double-band character of the two new bands (Figure 1) was also noted and has been discussed in detail in our previous studies.[21] Two corresponding different adsorption modes were proposed to explain this phenomenon. According to the potential dependence of the spectral features, the high-frequency component has been assumed to be related to the adsorption of the ion pair $CN^-\cdots Li^+$.[21] Other surface-adsorbed cyanide ions may be surrounded by solvent molecules, resulting in the appearance of the 2115-cm^{-1} band.

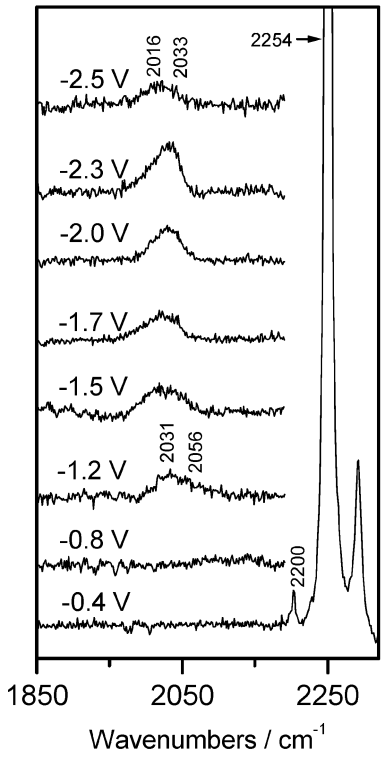

Figure 2. Representative potential-dependent SER spectra from a roughened platinum electrode in 0.1 M NaI/acetonitrile.

Iodide. Figure 2 shows the SERS spectra from a Pt electrode at different potentials after changing the electrolyte to 0.1 M NaI/CH_3CN. Unfortunately, the band reflecting the Pt−I interaction in the low-frequency region was not observed, which is possibly due to the rather low detection sensitivity for such an intermolecular vibrational mode. However, the adsorption of the iodide ion can be deduced by the spectral features presented in the CN stretching-mode region. As can be seen from Figure 2, the appearance of the CN^- band occurs at more negative potentials, namely, at −1.2 V, in comparison with the system without the addition of iodide (Figure 1). This clearly shows that the decomposition reaction of acetonitrile was inhibited significantly by changing the electrolyte to sodium iodide. Hence, we assume that there may be some blocking factors that occupy the surface decomposition reaction-active sites, most probably the kinks, edges, and steps of the Pt surface, which were originally associated with the solvent acetonitrile molecules. In the system used in Figure 1, these reaction-active sites were occupied by acetonitrile and subsequently facilitated its dissociation adsorption. As a result, it is reasonable to assume that the specific adsorption of iodide ions or related ion pairs onto the Pt surface reaction-active sites may be the main cause of the inhibition of acetonitrile decomposition. Certainly, the solvent molecules may also adsorb onto Pt surface sites other than the reaction-active ones. However, these site-associated solvent molecules should not decompose, or they decompose at a rather low speed or in a quantity that is below the detection limit of Raman spectroscopy.

The effort to measure the SERS features of adsorbed acetonitrile failed. The characteristic band observed at 2254 cm^{-1} at all potentials that were investigated (Figure 2, similar band features were omitted at potentials other than −0.4 V for clear presentation) corresponds to the CN triple-bond stretch of bulk solvent acetonitrile. However, the SERS spectra of acetonitrile has been observed on a roughened silver electrode by Irish and co-workers.[24] With the onset of the decomposition,

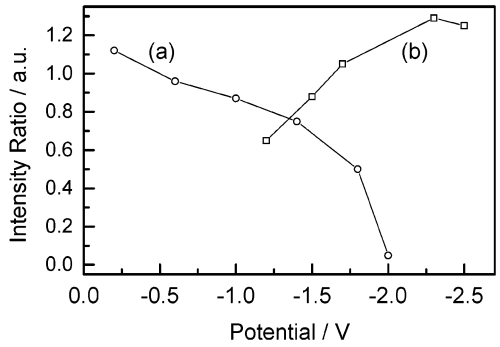

Figure 3. Potential dependence of the ratio of the band intensity for (a) 2147 cm^{-1}/2115 cm^{-1} with $LiClO_4$ as the electrolyte and (b) 2056 cm^{-1}/2031 cm^{-1} with NaI as the electrolyte. (See the text for a detailed description.)

the decrease in the CN-band intensity of acetonitrile can be clearly observed in their studies. This supports the dissociation of acetonitrile at roughened silver surfaces at negative potentials. In the present study, there is the possibility that the SERS band of acetonitrile is rather weak and that it may underlie the intense bulk solvent bands. Exactly those bands with different and well-resolved band frequencies, such as the CN^- band, would be expected to be apparently observable. Although we applied a subtraction method to the spectra, no obvious SERS bands of acetonitrile could be seen. This is reasonable because of the rather low surface enhancement factor (SEF) of the Raman signal for platinum (10−120). Moreover, the SEF further decreases by a factor of ca. 10 for platinum when using nonaqueous solvents in comparison with the widely used aqueous systems.[31]

All of these spectra show that the adsorption of iodide ions or related ion pairs onto the surface reaction-active sites greatly inhibits the decomposition of acetonitrile. No direct interaction of acetonitrile with the surface reaction-active sites would be expected at potentials positive to −1.2 V. Then, the acetonitrile molecule would be expected to adsorb via the methyl group with I^-, resulting in a difficult electron transfer between the metal substrate and acetonitrile. The possible direct interaction of acetonitrile with surface sites other than the reaction-active sites also does not facilitate the dissociation of acetonitrile. Thus, it is reasonable to assume that the adsorption of iodide significantly inhibits the decomposition reaction of the solvent in the vicinity of the electrode surface. This phenomenon has also been observed on a silver electrode.[24] When the potential is changed to sufficiently negative values, the iodide ion desorbs partially or completely from the surface because of the electrostatic repulsion of the negatively charged surface, and solvent decomposition then occurs. Additionally, the wide potential range observed for the adsorption of the product cyanide ion (Figure 2) may be indicative of a stronger interaction with Pt than with both iodide and the solvent.

Another interesting feature in Figure 2 is the reappearance of the double-band character for the CN stretching mode, namely, at 2031 and 2056 cm^{-1} at −1.2 V. This again can be explained by the existence of two types of surface ion pairs: $CN^-\cdots Na^+$ and $CN^-\cdots CH_3CN$. However, careful examination of the spectral features in Figures 1 and 2 shows that there is a difference in the potential dependence of the relative band intensity of the two bands. Figure 3 compares the relationship between the applied potential and the ratio of the band intensity with the higher frequency to that with the lower frequency. As can be seen from the Figure, the ratio value changes with potential in two different directions. The electrolyte anions of

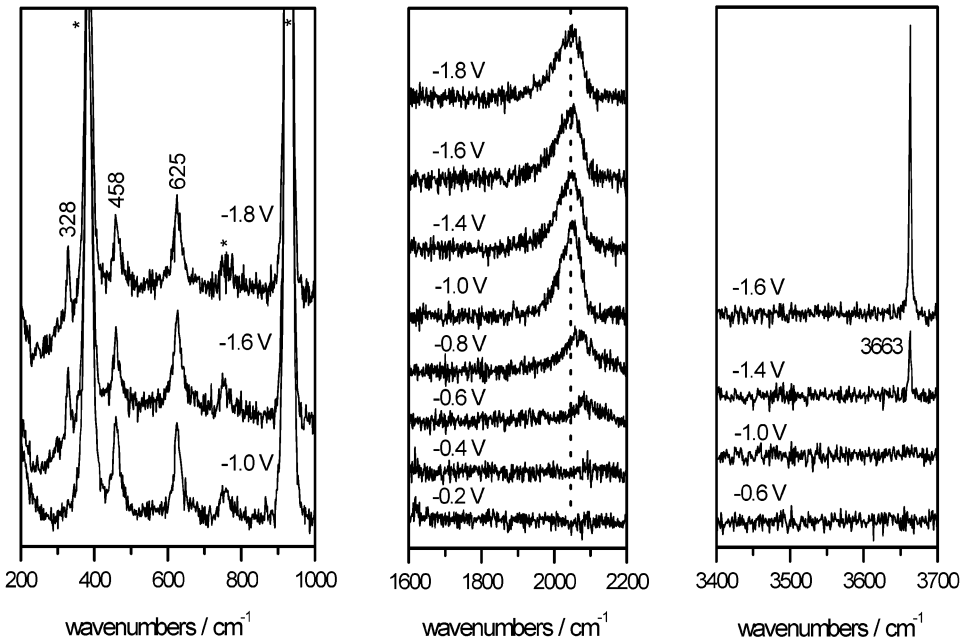

Figure 4. Representative potential-dependent surface Raman spectra from a roughened platinum electrode in acetonitrile with saturated $LiClO_4$ in three frequency regions: 200−1000 cm^{-1}, 1600−2200 cm^{-1}, and 3400−3700 cm^{-1}. Asterisks refer to the solvent bands.

ClO_4^- and I^- would be expected to have little effect on this observation because they possibly desorb from the surface in the potential region where the adsorption of CN^- occurs. As a result, the different behaviors of the relative intensity of the above two bands upon variations in the potential may be caused by the existence of different cations in the double-layer region.

It is reported that the potential of zero charge (pzc) for a platinum electrode in a neutral aqueous solution is around −0.2 to 0 V (vs SCE).[32] Although we have no accurate data for Pt, with $Hg/NaClO_3$ the pzc shifts 0.18 V in the negative direction from the aqueous to the CH_3CN solution.[33] Hence, we expect the pzc of Pt/CH_3CN to be shifted by a similar amount (i.e., at about −0.38 to −0.18 V (vs SCE). In the presence of the iodide ion, the pzc may further shift with a slightly negative value. On the basis of these assumptions, the adsorption of cyanide species should occur at negatively charged surfaces in the above two systems studied. This facilitates the adsorption of sodium or lithium cations, thus supporting the existence of ion pairs at the surface in the whole potential region where the adsorption of CN^- occurs.

When the potential is moved to more negative values, more cations (for instance, sodium cations in Figure 2) will be attracted to the vicinity of the surface, resulting in an increase in the relative intensity of the band associated with the ion pair, $CN^-\cdots Na^+/Li^+$. As a result, the increase upon the negatively going potential regarding the relative intensity of the 2056-cm^{-1} over the 2031-cm^{-1} band is observed (Figure 3). For the system with the lithium cation, there should be another contributing factor having the opposite effect. We will show in the later part of this paper that the trace water existing in the double-layer region may decompose while applying negative potentials to the electrode; the resulting OH^- then combines with Li^+, yielding the deposition of LiOH on the surface. Because of the rather low solubility of LiOH in acetonitrile, the normal Raman scattering of the stretching band arising from the combined OH^- can be detected, as presented later in Figure 4. On the basis of these observations, the formation of LiOH may be the main reason for the decrease in the intensity of the 2147-cm^{-1} band associated with the $CN^-\cdots Li^+$ ion pair at more negative potentials. Additionally, the yielding of insoluble LiOH layers covering the Pt surface may destroy part of the SERS-active sites. This is in agreement with the observations of the relatively low signal-to-noise ratio (S/N) in comparison with that in Figure 2.

Lithium Cation. The above results show that the cation in the double-layer region plays an important role in the surface adsorption process. We estimated that it should also have some effect on the surface structure of the double layer at the nonaqueous platinum−acetonitrile interface. Considering this assumption, a saturated electrolyte of $LiClO_4$ in acectonitrile was used in following SERS measurements to probe the role of the lithium cation in surface configurations.

Figure 4 shows a typical set of SERS spectra from a roughened Pt electrode at different potentials in such a solution. The spectra were presented in three frequency regions: 200−1000, 1600−2200, and 3400−3700 cm^{-1}. The applied potential was varied from positive, near the open-circuit potential of the system, to negative values. The bands marked with an asterisk correspond to the vibration of the bulk solvent. Additional bands observed at 458, 625, and 933 cm^{-1} come from the perchlorate anion in the bulk solution. As discussed in the Iodide section, the competitive adsorption of the lithium cation with the solvent molecule can also be deduced by the negative shift of the initial onset potential of the acetonitrile decomposition (from −0.2 to −0.6 V, see Figures 1 and 2). Because of the presence of saturated $LiClO_4$ in solution, a large quantity of Li^+ may transfer to the vicinity of the Pt surface even at potentials slightly negative to the pzc of the system, namely, from −0.2 to −0.4 V. The decomposition of the solvent would occur at more negative potentials. By contrast, the negative shift value of the onset potential for the present system (ca. 400 mV) is less than that with the addition of iodide ions (ca. 1000 mV, see Figure 2). Additionally, the disappearance of the double-band character appearing in Figures 1 and 2 can also be explained by the existence of a large number of Li^+ in the double-layer region. It is reasonable to assume that almost all of the adsorbed CN^- anions are surrounded by lithium cations. Only one type of ion pair, $CN^-\cdots Li^+$, is expected to exist at the electrode surface, resulting in the appearance of a single band of the CN vibration.

Another striking feature in Figure 4 is observed for the

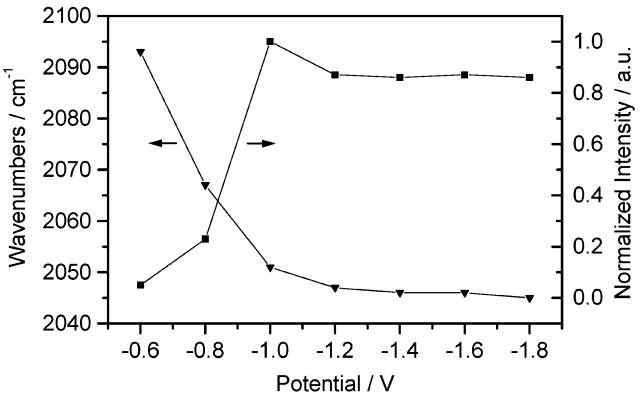

Figure 5. Potential dependence of the intensity and frequency of the CN^- band in acetonitrile with saturated $LiClO_4$ (see text).

changing of the CN^- band intensity and frequency upon variations in potential, as presented in Figure 5. The band intensity has been normalized. It can be seen from the Figure that the CN^- band first increases in intensity and then reaches its maximum at ca. −1.0 V, followed by a slight decrease then remaining almost constant at potentials negative to −1.4 V. The frequency of this band shifts to lower values first but is then constant at more negative potentials. It seems that the applied potential has no effect on the CN^- band, particularly at potentials negative to −1.4 V. More interestingly, this phenomenon was accompanied by the appearance of two new bands located at ca. 328 and 3663 cm^{-1} in lower- and higher-frequency regions, respectively. The band at 3663 cm^{-1} is extremely narrow with a fwhm (full width at half-maximum) of 6 cm^{-1}. Taking into account the possible existence of trace water in acetonitrile, the decomposition of water molecules would be expected to occur at a more negative potential. The adsorption of water molecules in acetonitrile has been confirmed on silver.[34] Unfortunately, the characteristic band of the adsorbed water molecule was not observed in the present study. This is possibly due to the rather low detection sensitivity, particularly in the high-frequency region for Pt compared with silver.

Therefore, the band at 3663 cm^{-1} may be related to the adsorbed water molecules. However, the rather high frequency and narrowness may reflect very little hydrogen bonding. On the basis of these observations, it is reasonable to postulate that the 3663-cm^{-1} band should arise from the product of water decomposition, the hydroxide anion. As described above, OH^- subsequently combines with the lithium cation, yielding an insoluble overlayer of LiOH at the Pt surface. The assignment of OH^- is in accordance with the peak position reported in the literature.[35,36] The normal Raman spectra of solid LiOH and $LiOH{\cdot}H_2O$ have OH^- stretching modes at 3664 and 3563 cm^{-1}, respectively,[35,36] supporting the above assignment. Although no characteristic band of hydrated LiOH was observed, the presence of this species may not be ruled out because the band is possibly weak. Additionally, it is reported that LiOH crystals have a layered structure, $(OH^-)_n Li^+_{2n}(OH^-)_n$,[37] so it is possible that such a structure forms in layers at the Pt surface. The relatively intense and narrow band observed at 328 cm^{-1} in the low-frequency region is probably from the crystal lattice vibration of LiOH, supporting the formation of LiOH at the surface. Such a LiOH crystal layer was also observed in the Ag/acetonitrile system.[24]

On the basis of the above assignments, the behavior of the CN^- band with respect to applied potential can be explained as follows. As discussed in our previous study,[21] the red shift of the frequency of the CN band upon variations in potential is mainly caused by the electron transfer between the adsorbate and Pt (i.e., the electrochemical Stark tuning effect).[38,39] Briefly, CN^- has one electron sitting on its weak 5σ antibonding orbital.[40] When the potential is moved to a positive value compared to the pzc of the Pt electrode, the electron density of this orbital will be reduced, leading to an increase in the frequency of the CN band. On scanning the potential to negative values, the electrode surface donates electrons to the 5σ antibonding orbital of CN^-, resulting in a weakening of the CN bond and hence a decrease in frequency. In the present study, the variation of the CN band frequency at potentials positive to ca. −1.4 V is in good accordance with the Stark tuning effect. When the potential is altered to more negative values, the formation of an overlayer of LiOH would be expected to inhibit the electron transfer between Pt and the CN^- anion. In other words, the vibronic structure of the overlayer-adsorbed CN^- is not sensitive to the change in the applied potential, resulting in an almost constant frequency of the CN band. However, the deposition of CN^- in the surface crystal lattice of LiOH is also reasonable. Thus, the relatively intense CN band observed at potentials negative to ca. −1.4 V in comparison with Figure 1 may not arise from the direct metal−CN^- interaction but from normal Raman scattering of the inbuilt CN^- in the LiOH crystal lattice. Therefore, the intensity of this band should be determined by the quantity of the inbuilt CN^-. However, the assumption of the inbuilt CN^- in the LiOH crystal lattice should be further confirmed by other techniques. The spectral features in Figure 4 indicate that the quantity of CN^- existing at the interface may be constant in the potential region negative to −1.4 V. Therefore, no further decomposition of acetonitrile would occur in the same potential region because of the covering of the LiOH layer on the Pt surface. However, the growth of the LiOH layer continues, as evidenced by the increase in the intensity of the 328- and 3663-cm^{-1} bands, indicating continuing water decomposition at the Pt surface.

Water. The above discussions suggest the existence of trace water in the electrochemical double-layer region of the Pt/acetonitrile system because the utter remove of trace water from the solvent is difficult to realize. Probing of the possible competitive adsorption of water and acetonitrile was then performed by adding water to the solution used in Figure 1. The corresponding SERS spectra from the same roughened Pt electrode at different potentials in 0.1 M H_2O + 0.1 M $LiClO_4$/CH_3CN are presented in Figure 6. Again, the competitive adsorption of the water molecule could be anticipated. As seen from the Figure, the onset potential of acetonitrile decomposition is shifted in a negative direction to −0.7 V by ca. 500 mV in comparison with that in Figure 1 but is comparable to that in Figure 4. This may suggest the predominance of water molecules in the vicinity of the electrode surface at relatively positive potentials, which inhibits the approach of the solvent molecule to the surface, particularly those reaction-active sites for the decomposition of acetonitrile. Unfortunately, direct evidence of the SERS bands from interfacial water was not obtained. This may be caused by both the rather low detection sensitivity and the rather small Raman scattering cross section for water molecules. However, because of the great enhancement of the surface Raman signal for silver, the SERS bands of trace water have been observed at the roughened silver electrode−acetonitrile interface in our laboratory.[41]

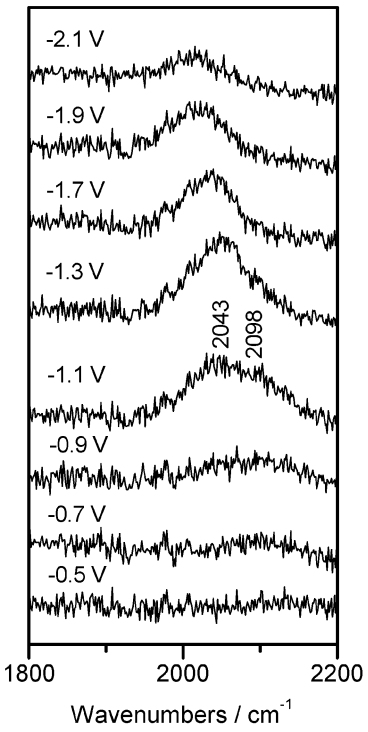

Figure 6. SERS spectra from a roughened Pt electrode at different potentials in 0.1 M H_2O + 0.1 M $LiClO_4$/acetonitrile.

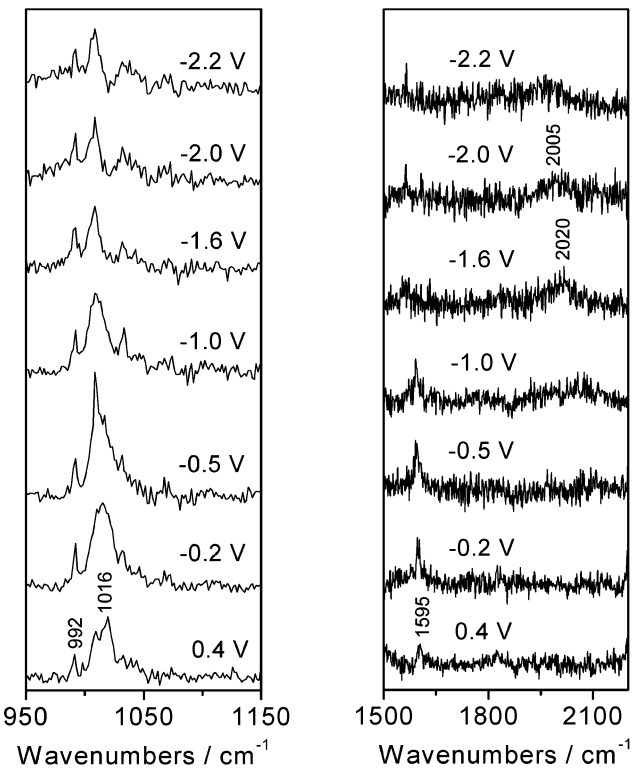

Figure 7. Typical set of potential-dependent surface Raman spectra from a roughened platinum electrode in 0.1 M pyridine + 0.1 M $LiClO_4$/acetonitrile in two frequency regions: 950−1150 and 1500−2150 cm^{-1}.

The spectral feature in Figure 6 again gives the double-band character of the CN mode. This can also be explained by the existence of two ion pairs at the surface: $CN^-\cdots Li^+$ and $CN^-\cdots CH_3CN$. Additionally, the intensity of the two bands exhibits a similar potential dependence to that in Figure 1. This may suggest a similar effect of the lithium cation on the adsorption of the CN^- anion. A difference is also observed for the two systems. The CN band is widened, particularly at relatively positive potentials (for instance, at −1.1 V; Figure 6). This may be caused by the contributions from the interaction of water with adsorbed CN^-.

By comparing the negative shift of the onset potential of acetonitrile decomposition upon the addition of water, the lithium cation, and iodide, we estimate a stronger surface interaction of iodide with Pt than with both the water molecule and the lithium cation. This is in accordance with the specific adsorption property for halide ions, irrespective of the use of an aqueous or nonaqueous solution.

Pyridine. Now we choose pyridine, a typical heterocyclic adsorbate on metallic surfaces and widely used as the probing molecule in SERS studies, as the present test molecule. Unlike the water molecule with a small Raman scattering cross section, the pyridine molecule has large cross-sectional value and is hence estimated to exhibit SERS bands when added to the present Pt/acetonitrile system.

Figure 7 shows a typical series of potential-dependent SER spectra of pyridine adsorbed onto a roughened platinum electrode in 0.1 M pyridine + 0.1 M $LiClO_4$/acetonitrile. The spectra are presented in the frequency ranges of 950−1150 cm^{-1} and 1500−2150 cm^{-1}. The applied potential is varied from positive to negative. As can be seen from the Figure, the band centered at ca. 1016 cm^{-1} from pyridine is well resolved. A change in the frequency of this band upon adsorption is also clearly observed, suggesting that the 1016-cm^{-1} band attributed to the symmetric ring-breathing mode of pyridine[42] is from the surface species rather than the bulk solution. The band observed at 992 cm^{-1} is caused by the interference of the bulk pyridine because of the use of a relatively high concentration of pyridine. Two other bands, located at ca. 1031 and 1595 cm^{-1}, are also observed and are ascribed to the asymmetric ring-breathing and ring-stretching modes, respectively.[42]

The intensity of the symmetric ring-breathing mode first increases to a maximum value at ca. −0.5 V and then remains almost constant when the potential is changed to more negative values. In comparison with SERS of pyridine in aqueous media,[14] the potential region where pyridine adsorption occurs is extended greatly from about 1.4 to >2.6 V (Figure 7). This may be attributed to the elimination of the hydrogen-evolution reaction at the negative potential limit in the present system. It again shows the advantage of using an organic solvent over the aqueous solution.

The CN^- band normally observed in several of the former systems is hardly detected at potentials positive to ca. −1.6 V (Figure 7). Only when the electrode is polarized at ca. −1.6 V can the CN^- band be resolved. Moreover, the S/N ratio is rather poor, suggesting a rather small number of adsorbed cyanide ions at the Pt surface. On the basis of these observations, we postulate that the strong adsorption of pyridine on Pt significantly impedes direct interactions of the solvent molecule with the surface reaction-active sites. As discussed above, the surface reaction-active adsorption sites would be occupied by pyridine molecules over a wide potential region. Hence, the solvent acetonitrile could hardly exhibit decompositions because of the difficulty of electron transfer. The surface-activation properties of pyridine molecules in acetonitrile are then clearly concluded.

In comparison with the former three systems studied, the adsorption ability of pyridine at the Pt−acetonitrile interface would be the strongest. The interactions of these molecules/ions with Pt are assumed to decrease as follows: pyridine > I^- > water ≈ Li^+.

Summary

The electrochemical Pt−nonaqueous acetonitrile solution interface in the presence of iodide, the lithium cation, water, and pyridine molecules, respectively, was examined as a function of applied potential employing surface-enhanced Raman spectroscopy (SERS). The special roughening pretreatments of the Pt electrode helped us to obtain high-quality Raman signals. The main observations and conclusions have been summarized:

(1) Surface-enhanced Raman scattering from a roughened Pt electrode in acetonitrile is reported. Two new bands observed at ca. 2115 and 2147 cm^{-1} were observed and attributed to adsorbed CN^- surrounded by solvent molecules and lithium cations, respectively.

(2) The competitive adsorptions of iodide, the lithium cation, water, and pyridine with the solvent acetonitrile were confirmed and analyzed on the basis of measured spectra. It was postulated that the solvent acetonitrile molecules, particularly those associated with surface reaction-active sites, may be replaced by I^-, water, and pyridine molecules when added to the solution, which shifts the onset potential of acetonitrile decomposition to more negative values. When used at a saturated concentration, the lithium cation also has an inhibiting effect on this decomposition reaction.

(3) For the systems with water or iodide, double-band character for the CN band was observed. It is assumed to be due to the existence of two types of adsorbed ion pairs at the Pt surface: $CN^-\cdots CH_3CN$ and $CN^-\cdots Li^+/Na^+$.

(4) In the presence of pyridine, the decomposition of acetonitrile was almost completely suppressed by the strong interaction of pyridine with the Pt surface. According to the different negative shift values of the onset potential of this decomposition reaction for the systems with iodide, water, or the lithium cation, the interactions of these adsorbates with Pt are assumed to weaken as follows: pyridine > I^- > water ≈ Li^+.

Acknowledgment. This work was supported by the Natural Science Foundation of China and the State Key Laboratory for Physical Chemistry of Solid Surfaces of Xiamen University. The Raman spectroscopy experiments were carried out at Xiamen University. We are grateful for the kind help of coworkers there.

References and Notes

(1) Fleischmann, M.; Hendra, P. J.; Mcquillan, A. J. *Chem. Phys. Lett.* **1974**, *26*, 163.
(2) Jeanmaire, D. L.; VanDuyne, R. P. *J. Electroanal. Chem.* **1977**, *84*, 1.
(3) Albrecht, M. G.; Creighton, J. A. *J. Am. Chem. Soc.* **1977**, *99*, 5215.
(4) Campion, A.; Kambhampati, P. *Chem. Soc. Rev.* **1998**, *27*, 241.
(5) Hutchinson, K.; Mcquillan, A. J.; Hester, R. E. *Chem. Phys. Lett.* **1983**, *98*, 27.
(6) Pemberton, J. E.; Bryant, M. A.; Sobocinski, R. L.; Joa, S. L. *J. Phys. Chem.* **1992**, *96*, 3776.
(7) Deng, Z. Y.; Irish, D. E. *J. Phys. Chem.* **1994**, *98*, 9371.
(8) Mengoli, G.; Musiani, M.; Fleischmann, M.; Mao, B. W.; Tian, Z. Q. *Electrochim. Acta* **1987**, *32*, 1239.
(9) Uehara, J.; Nishihara, H.; Aramaki, K. *J. Electrochem. Soc.* **1990**, *137*, 2677.
(10) Oblonsky, L. J.; Devine, T. M.; Ager, J. W.; Perry, S. S.; Mao, X. L.; Russo, R. E.; *J. Electrochem. Soc.* **1994**, *141*, 3312.
(11) Zou, S.; Williams, C. T.; Chen, E. K.-Y.; Weaver, M. J. *J. Am. Chem. Soc.* **1998**, *120*, 3811.
(12) Zou, S.; Weaver, M. J.; Li, X. Q.; Ren, B.; Tian, Z. Q. *J. Phys. Chem. B* **1999**, *103*, 4218.
(13) Luo, H.; Weaver, M. J. *Langmuir* **1999**, *15*, 8743.
(14) Ren, B.; Huang, Q. J.; Cai, W. B.; Mao, B. W.; Liu, F. M.; Tian, Z. Q. *J. Electroanal. Chem.* **1996**, *415*, 175.
(15) Cao, P. G.; Yao, J. L.; Ren, B.; Gu, R. A.; Tian, Z. Q. *Chem. Phys. Lett.* **2000**, *316*, 1.
(16) Huang, Q. J.; Li, X. Q.; Yao, J. L.; Ren, B.; Cai, W. B.; Gao, J. S.; Mao, B. W.; Tian, Z. Q. *Surf. Sci.* **1999**, *427−428*, 162.
(17) Cao, P. G.; Yao, J. L.; Zheng, J. W.; Gu, R. A.; Tian, Z. Q. *Langmuir* **2002**, *18*, 100.
(18) Cao, P. G.; Yao, J. L.; Ren, B.; Gu, R. A.; Tian, Z. Q. *J. Phys. Chem. B* **2002**, *106*, 7283.
(19) Cao, P. G.; Sun, Y. H.; Yao, J. L.; Ren, B.; Gu, R. A.; Tian, Z. Q. *Langmuir* **2002**, *18*, 2737.
(20) Larson, R. C.; Iwamoto, R. T.; Adams, R. N. *Anal. Chim. Acta* **1961**, *25*, 371.
(21) Gu, R. A.; Cao, P. G.; Sun, Y. H.; Tian, Z. Q. *J. Electroanal. Chem.* **2002**, *528*, 121.
(22) Cooney, R. P.; Fraser, D. B. *Aust. J. Chem.* **1974**, *27*, 1855.
(23) Ren, B.; Li, X. Q.; Wu, D. Y.; Yao, J. L.; Xie, Y.; Tian, Z. Q. *Chem. Phys. Lett.* **2000**, *322*, 561 and references therein.
(24) Irish, D. E.; Hill, I. R.; Archambault, P.; Atkinson, G. F. *J. Solution Chem.* **1985**, *14*, 221.
(25) Mernagh, T. P.; Cooney, R. P. *J. Electroanal. Chem.* **1984**, *177*, 139.
(26) Ou, E. C.; Young, P. A.; Norton, P. R. *Surf. Sci.* **1992**, *277*, 123.
(27) Villegas, I.; Weaver, M. J. *J. Am. Chem. Soc.* **1996**, *118*, 458.
(28) Roth, J. D.; Chang, S.-C.; Weaver, M. J. *J. Electroanal. Chem.* **1990**, *288*, 285.
(29) Anderson, M. R.; Huang, J. *J. Electroanal. Chem.* **1991**, *318*, 335.
(30) Dederichs, F.; Petukhova, A.; Daum, W. *J. Phys. Chem B* **2001**, *105*, 5210.
(31) Cao, P. G.; Gu, R. A.; Ren, B.; Tian, Z. Q. *Chem. Phys. Lett.* **2002**, *366*, 440.
(32) *Encyclopedia of Electrochemistry of the Elements*; Bard, A. J., Ed.; Marcel Dekker: New York, 1976; Vol. 6.
(33) Yamashita, K.; Imai, H. *Bull. Chem. Soc. Jpn.* **1977**, *50*, 1066.
(34) Gu, R. A.; Sun, Y. H.; Cao, P. G.; Cao, W. D.; Yao, J. L.; Ren, B.; Tian, Z. Q. *Acta Chim. Sin.* **2001**, *59*, 1522.
(35) Hase, Y.; Yoshida, I. V. P. *Chem. Phys. Lett.* **1979**, *65*, 46.
(36) Phillips, B. A.; Busing, W. R. *J. Phys. Chem.* **1957**, *61*, 502.
(37) Bredig, M. A. *J. Chem. Phys.* **1956**, *24*, 1037.
(38) Zou, S.; Weaver, M. J. *J. Phys. Chem.* **1996**, *100*, 4237.
(39) Lambert, D. K. *Electrochim. Acta* **1996**, *41*, 623.
(40) Daum, W.; Dederichs, F.; Muller, J. E. *Phys. Rev. Lett.* **1998**, *80*, 766.
(41) Cao, P. G.; Gu, R. A.; Qiu, L. Q.; Sun, R.; Ren, B.; Tian, Z. Q. *Surf. Sci.* **2003**, *531*, 217.
(42) Dollish, F. R.; Fateley, W. G.; Benley, F. F. In *Characteristic Raman Frequencies of Organic Compounds*; Wiley: New York, 1974.